Automatic Generation and Population of a Graphics-Based Driving Simulator

Use of Mobile Mapping Data for Behavioral Testing of Drivers

Michael Brogan, David Kaneswaran, Sean Commins, Charles Markham, and Catherine Deegan

A stereo image and high-accuracy positional data were used to generate and populate a low-fidelity graphics model. The data were acquired by a simple mobile mapping system. The use of positional data made it possible to generate automatically a sparse model consisting of a road, central road marking, a green area, and a skybox. This allowed for several applications, such as the synchronization of the model with the video and the semiautomatic population of road signs into the model data. An experiment was conducted to evaluate the model and the video as viable sources for behavioral testing of drivers. The correlations between driver speed in response to the model and the video are presented; this presentation allows for an examination of the effect of the fidelity of the driving simulator's visual cue stream. The study results were used to compare driver speed in a real vehicle with driver speeds in the video and model roads, with correlations of 84.6% (between video and ground truth), 87.3% (between model and ground truth), and 92.8% (between video and model).

Driving simulation has evolved from its earliest incarnation of a driving cab placed in front of a painting of a road scene to the computer age and the generation of virtual worlds that allow for a steerable environment where programmable scenarios can be introduced (*1*). Rapid advancements in computer technology and digital imaging techniques mean that photo-realistic models of 3-D environments are becoming more common (*2, 3*).

A desire to replicate real roads has led to the development of driving simulators that afford the user the ability to drive modeled environments of world routes alongside other simulators that attempt to model road design problems (*4–8*). Several virtual representations of world routes exist, and although they are being developed to ever-increasing levels of fidelity, they remain virtual (*9*).

Generation of geometrically accurate, 3-D environments generally requires the use of multicamera setups in combination with a lidar device (*10*). These typically generate large amounts of data and have a high cost. Although lower-cost devices, such as the Microsoft Kinect, can be used to generate photo-realistic models of environments, they are constrained in terms of the amount of spatial data that can be reconstructed (*2*). Other methods of constructing geoaccurate models include the analysis of existing Geographic Information System (GIS) data. Although those analyses produce geoaccurate models, they lack information from the GIS data to introduce road traffic signs and other nongeometric, road-specific features (*11*).

The popularization of geoaccurate mapping data has become more widespread in recent years, with the launch and subsequent rise in popularity of enterprise-funded GIS systems, such as Google Earth, and crowd-sourced data, such as Open Street Map (*12, 13*). These data sources have been used to construct basic driving simulator models for behavioral testing and general gaming purposes (*14, 15*).

Other research has attempted to introduce photo-realistic elements into driving simulation by generating a hybrid of model and photo, whereby objects in the distance were represented to the driver by way of photographs and objects closer to the driver were represented by models (*16*). State-of-the-art research has integrated lidar reconstructed models with photographic textures to generate photo-realistic environments, although no information is presented on the effect of the increased fidelity provided to the driver (*17*). The method presented in Bredif allows for the accurate reconstruction of urban-based environments, as the lidar data used as its base model allow for the texturing of well-defined geometric models, such as buildings (*17*). However, it is unclear how the same texture mapping would result in a rural environment, where sometimes the only well-defined geometric model is that of the road.

The monitoring of driver behavior is a common task assigned to research simulators as the recording of many aspects of driver behavior, such as eye gaze, speed, braking response, and distraction effects, is achievable (*18–21*). A comparison of the braking response of drivers in a simulator compared with their response on a test track found that validation of driver simulator data is important and acknowledged that direct validation is difficult (*21*).

Driving simulator evaluation consists of three general stages, namely, transferability, reliability, and validity (*22*). For a driving simulator to be considered valid, it should at least allow for the transference of basic driving skills (*22*). Similarly, reliability should be examined as part of the evaluation process, as a simulator subsystem can be reliable but also incorrect. For example, when considering

M. Brogan and C. Deegan, Department of Engineering, Institute of Technology Blanchardstown, Dublin 15, Ireland. D. Kaneswaran and C. Markham, Department of Computer Science; and S. Commins, Department of Psychology, National University of Ireland, Maynooth, County Kildare, Ireland. Corresponding author: M. Brogan, michael.brogan@live.ie.

Transportation Research Record: Journal of the Transportation Research Board, No. 2434, Transportation Research Board of the National Academies, Washington, D.C., 2014, pp. 95–102.
DOI: 10.3141/2434-12

a flaw in the braking subsystem that provides consistent but nonetheless erroneous results, the so-called reliable results are rendered incorrect. The validity of a test can be defined as how well the test measures that which it was designed to measure (*22*). Validation is achieved, when a test measures accurately that which it is supposed to measure.

Allen et al. state that a comparison of simulator behavior with real-world results obtained under uncontrolled observable conditions might be regarded as the highest form of validation (*23*). The same research stated that validation for a single aspect of simulator usage cannot be considered validation for the entire simulator. For example, a validated speed production simulator may lack the monitor resolution to serve as a valid road sign simulator (*23*).

Driving simulation can be considered to consist of the engagement of four primary sensory component interactions: visual, auditory, proprioception, and vestibular. Validation experiments may be required for one or a combination of all four, depending on which aspect of driving simulation is to be validated (*23*).

PRINCIPAL FINDINGS

The driving simulator described in this paper used a high-accuracy, time-stamped, and geo-tagged stereo video of a real-world route. The route was acquired by a real driver on a real road under normal driving conditions as a basis to generate an accurate 3-D model. This was achieved through the use of positional data describing the trajectory of the vehicle at the time of data acquisition. The video acquired was in stereo format, thereby allowing the depth of features relative to the camera to be calculated, enabling the semiautomatic population of the model with features such as road signs. In addition to the automatic generation and semiautomatic population of a model, the video can also be synchronized with the model. This allows for a driver to control progression through both the video and the model in an identical fashion; for example, traveling at 50 km/h (31 mph) for 30 s will advance both to the same location along the route.

As both the video and the graphical model were acquired or generated through the use of the same GPS coordinate log, synchronization between the two was achievable; a participant was able to move through both the model and the video at the same time and at the same speed and was at the same position along the route in the model and the video.

An evaluation experiment was undertaken to examine the relationship among the ground truth, the graphical model, and the video. This allowed for testing driver response in terms of speed across the entire route. As the model and video were synchronized and the model was populated with road signs based on the video, the study was able to compare the sparsely populated model with the video on the effect of the increase in visual fidelity on a driver. The results suggest that the increase in fidelity did not affect the driver's response in terms of speed. For the purposes of this study, the fidelity of the visual cue system was taken to mean the visual complexity of the system as presented to the driver.

The visual cue system alone was examined for the purpose of evaluating driver speed simulation, following the three stages of evaluation described by Blana (*22*):

- Transferability: the transfer of driver speed from the real world to the driving simulator,
- Reliability: consistency within each fidelity's data set, and
- Validity: comparison between the video and the model to find the extent to which the two visual cue streams are correlated.

FRAMEWORK

This paper describes the method by which the testing route was selected and the hardware used to form the Mobile Mapping System (MMS). The paper will describe the use of MMS to acquire stereo image data and high-accuracy positional data, allowing for a ground truth speed to be generated, representing the speed of a driver on the real road in a real vehicle. The process by which the positional data were used to generate a sparse graphical model is then described, along with a method combining this model with the image data to populate the model with road signage. The paper will present and discuss an experiment that evaluated a driver's response to the model and the video.

MATERIALS, METHODS, AND DATA

Driving Simulator Cabin and Primary Control System

The driving simulator used in the experiment consisted of a static, fixed-base cabin, incorporating a car seat reclaimed from an end-of-life vehicle. The driving simulator used a standard Microsoft Windows 7–based PC, with a Logitech G27 force-feedback steering wheel, pedals, and gear-stick as its primary control system (*24*). A Matrox TripleHead2Go was used to combine three standard 1280 × 1024 resolution monitors to produce a single 3840 × 1024 display (*25*). The driving simulator is shown in Figure 1.

FIGURE 1 Static, fixed-base driving simulator with triple-monitor setup.

Route Selection and Acquisition of Mapping Data

The route chosen for data acquisition was the R156 regional road in County Meath, Ireland. Road classification in Ireland is governed by the National Roads Authority, which designates roads in Ireland as local, regional, national, or motorway (*26*). The R156 was chosen as it offers a high degree of geometric sinuosity, along with various vehicle speed limit sections, that is, 50 km/h (31 mph), 60 km/h (37 mph), and 80 km/h (50 mph). The route is approximately 17.6 km (10.9 mi) in length and takes approximately 16 min to travel.

For the acquisition of the road image and navigational data, the MMS consisted of a stereo camera and a Real-Time Kinematic (RTK) correction streaming–enabled GPS receiver. RTK correction streaming employs several virtual base-stations to reduce the standard GPS error from ≈ 5 m (5.47 yd) to less than 5 cm (2 in.). The system is configured in such a way that the GPS receiver logs its position at a rate of 10 Hz and, upon the generation of each log, also triggers the stereo camera, thereby acquiring geo-tagged stereo images with accuracy greater than 5 cm (2 in.). The log generated by the GPS receiver is time-stamped, thereby allowing the distance and time between camera frames to be calculated. The stereo camera used by the acquisition system was the PGR Bumblebee XB3 stereo camera, used with a baseline of 24 cm (9.45 in.), and the RTK-enabled GPS receiver used was the NovAtel® Pro-Pak V3 (*27, 28*).

Use of Mapping System GPS Data for Generation of the Graphical Model

The GPS data acquired by the mapping system were used to form the basis for a graphics-based model environment. Superelevation was not implemented for this iteration of the driving simulator, as the road chosen was of an Irish regional category, normally driven at speeds lower than that of a highway. The only descriptors in the model are of the road, lines, signs, and green and sky areas. Superelevation data may be introduced into future iterations of the driving simulator by integrating the Inertial Measurement Unit data as acquired by the system at the time of mapping.

Implemented in Microsoft XNA Game Studio 4.0, the GPS trajectory was reordered and interpolated such that the route was regenerated as a sequence of evenly-spaced, 3-D points. This evenly spaced trajectory was used as the defining line, around which a sparse 3-D model was constructed.

As the mapping system traversed the road under normal driving conditions, this trajectory therefore estimated the center of the left road lane in Ireland. In the model, the driver was placed in the center of the left road lane. However, a deviation could have occurred on lane position in the video data. The positional data acquired by the mapping system were inspected for any major deviations from the center of the road lane by overlaying the GPS data on the Google Earth view of the same road. Careful choice of the video sequence was used to exclude large deviations caused by, for example, any overtaking maneuvers. This set of points could then be used as a basis to construct a polygon model. This is shown in Figure 2.

As the GPS trajectory describes the center of the left road lane, this approach for forming a polygon was extended in such a way that the equidistant points, w, x, y, and z, were translated so that they shifted the edge of the generated polygon by a predetermined value. This allowed 25% of the road polygon to be translated to the left of the vehicle trajectory and the remaining 75% to the right. This represents the estimated position of the vehicle on the real road. Once generated, the area surrounding the road was tiled with a green square and the entire model was contained in a skybox.

Following the generation of this sparse model, there are now two data sets that can be replayed with the driving simulator; namely, a low-fidelity model and a high-fidelity video, both representing the same real-world route. The model is viewed via a virtual camera, positioned at an initial (X, Y, Z) coordinate (1.50 m, 0.43 m, −15.00 m). As they represent the same route and both follow an identical trajectory, synchronization between the two is achievable, meaning that a participant can travel along both the model and the video. An accelerator pedal was used to control the rate of advancement through the model and the video. This synchronization was implemented through a look-up table, which was generated based on the current position of the camera view in the model along the route. By logging the distance traveled along the route, the nearest corresponding GPS coordinate and therefore the nearest corresponding image frame could be calculated. The result of this was a sparse 3-D model that was synchronized with a video representing the same real-world route. Any pressure applied to the driving simulator's accelerator pedal will advance through the model and the video at the same rate. An example of this synchronicity is shown in Figure 3.

Use of Mapping System Stereo Imaging Data to Populate the Graphical Model

Population of the model with road signs can be achieved in two ways: a manual method and a semiautomatic method. The manual method requires that a user display the model and video simultaneously. When a road sign is observed in the video, a road sign editor can be opened that allows a user to insert the sign manually; this road sign editor can be seen in Figure 4.

The semiautomatic method uses the stereo image data acquired by MMS. MMSs that use cameras as imaging sensors require a camera calibration routine that recovers the position and orientation of the

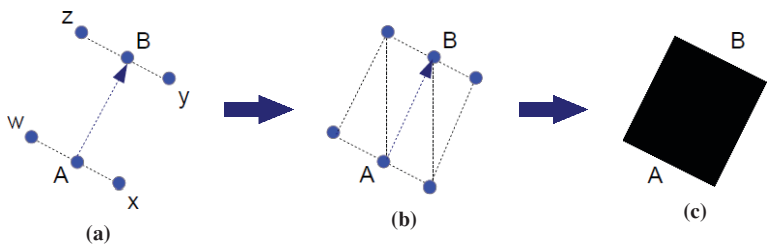

FIGURE 2 Construction of polygon from mapping system trajectory points: (*a*) Trajectory Points A and B and Equidistant Points w, x, y, and z; (*b*) generation of four polygons; and (*c*) filled-in polygons.

FIGURE 3 Example of synchronicity achieved between GPS trajectory-based model and video. Same bend is visible in both model and video. Speedometer is common to both, allowing a participant to move through both model and video at same time and at same speed.

camera relative to some arbitrary world coordinate system and also to each other (*29*). Calculation of the position of a feature can then be made with reference to this coordinate system or either of the cameras. However, any movement of the camera requires recalibration or a way to measure this movement. There are several methods for tracking this change in camera orientation. Inertial measurement units can be used to measure this change in terms of roll pitch and yaw angular deviations; visual odometry and the integration of GPS positional data can also be used to estimate a camera's orientation (*30–32*).

As the model is generated by use of GPS coordinates acquired by the mapping system and the model and video sequence are synchronized, any feature, such as a road sign, can be assigned a 3-D coordinate local to the left stereo camera (*29*). The left camera and the model camera are offset by the translation between the GPS receiver and the camera (the camera and GPS receiver were mounted collinear, with a 3.3-m offset in the camera's Z direction) and the initial (X, Y, Z) camera model view (1.50 m, 0.43 m, −15.00 m). Accounting for these allows the local camera coordinate to be transformed into the model's coordinate system.

This process has two benefits: the population of the model with road signs detected in the video and the georeferencing of the road signs by recovering their 3-D coordinates in the model. As the model is generated with the GPS data acquired by the mapping system, any feature inserted into the model can then be assigned a georeference. An example of this process is shown in Figure 4.

Because of factors such as the errors inherent in the calibration of mapping system cameras and the fact the road may not be of a constant width, as is typical of regional roads in Ireland, the calculated model coordinate may not lie in the precise location desired (*29*). To compensate for this, a model editor was introduced to allow for editing of the post-insertion coordinate. This is shown in Figure 5.

BEHAVIORAL TESTING OF DRIVERS

Eleven participants drove through both the video and model representations of the R156 route. The ages of the participants ranged from 19 to 47 years, with 10 males and one female. As the video does not allow for any control over the steering and as this evaluation experiment was designed to consider speed only, all forms of control were disabled except for the accelerator pedal. This was consistent in both the model and the video. The participants were informed of the control system before the experiment began. The instructions given to the participants were that the road segment began in a 60-km/h (37-mph) zone and that participants were to drive in a normal manner, responding to the road as if they were driving a real vehicle. Applying pressure to the accelerator pedal increased the rate at which the participant traveled along the route. Conversely, reducing pressure to the pedal slowed the rate. Each participant's speed at 0.1-m (3.94-in.) intervals along the route was recorded.

An output data file was produced for each participant in each visual cue type, consisting of 175,800 points (representing a total route distance of 17.58 km). The 175,800 points were reduced to

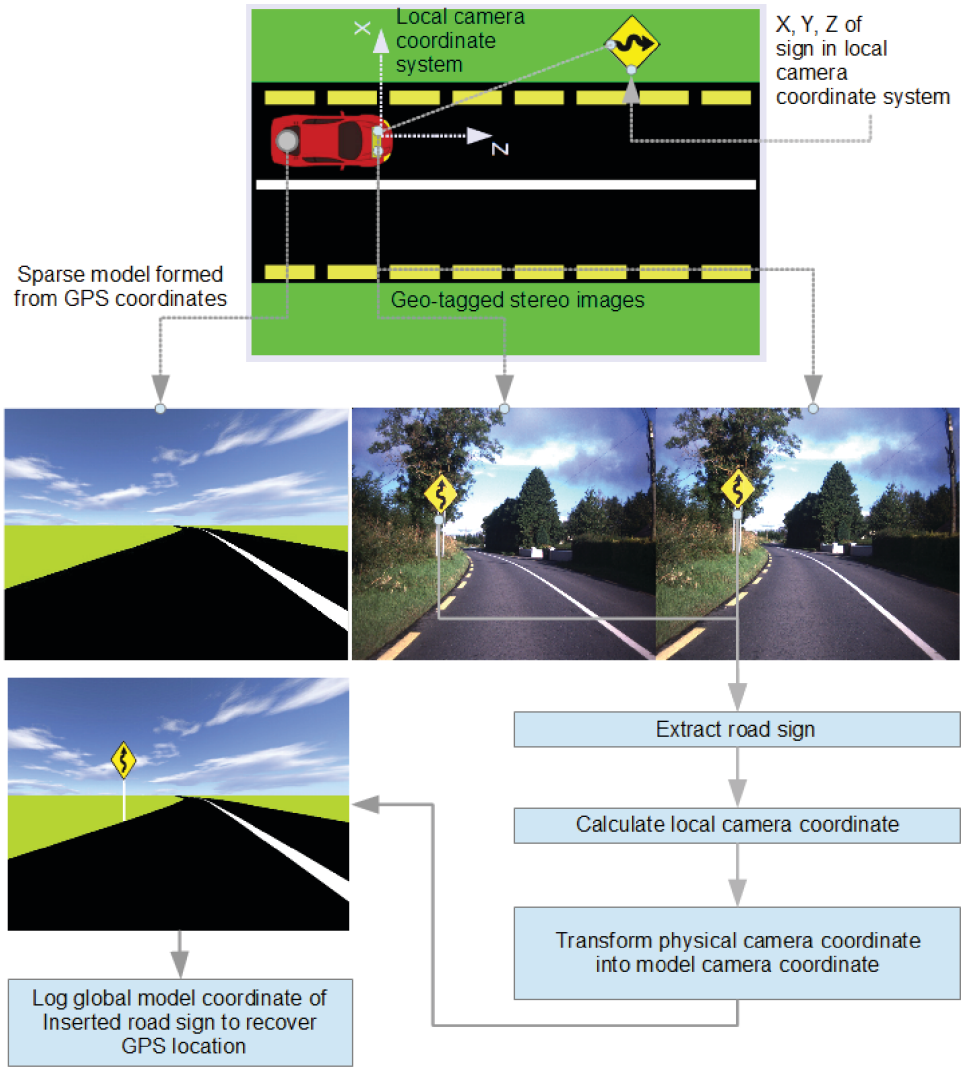

FIGURE 4 Example of population and georeferencing of road signs along the route. As model and video are synchronized, local coordinates of road sign in model are recoverable from stereo camera calibration data.

99 points, calculated as a running average, where each resultant point represents a distance of 177.58 m (0.11 mi). This process was repeated for the original mapping system ground truth speed data.

Each set of data (model, video, and ground truth) was then compared under the three evaluation components identified in McLoughlin et al.: transferability, reliability, and validity (*31*).

DISCUSSION OF RESULTS

The average values of the ground truth, video, and model are shown in Figure 6. The features at three locations that coincided with a decrease in speed are also shown. Error bars representing standard errors in the video and model results are included.

These results are discussed under the three evaluation criteria described in Blana (*22*). For the purposes of this paper, transferability is defined as the transfer of driver speed from the real world to the driving simulator. Reliability is interpreted as the consistency between participants in each of the visual cue streams. Validity is defined as the extent to which the simulator measures driver speed.

Transferability

Figure 6*a* shows a subset of road features that coincide with a decrease in speed among all three speed data sets (i.e., ground truth (Figure 6*b*), video (Figure 6*c*), and model (Figure 6*d*)). This shows that the speed of drivers in the driving simulator transfers from the real world to the simulator.

Drivers were told to drive as they would normally and that the starting segment had a posted speed limit of 60 km/h (37 mph). If the participants followed the posted speed limits only, no reduction in speed would have been observed when drivers entered bends; this result suggests that the participants reacted to the geometry presented to them, regardless of the fidelity.

FIGURE 5 Example of postinsertion editing of road sign placement: (*a*) updated local coordinates, (*b*) view of road, and (*c*) editor screen. Editor allows for the manipulation of the X, Y, and Z coordinates and also orientation of sign relative to road.

Several large differences in the speed between the ground truth data and the model or video data are observed at multiple locations throughout the route, although the driver of the mapping system acquisition vehicle drove normally and the mapping system required no special consideration when driving. A factor in the differences between the real-world and simulator data may have been the time taken to change gears of the manual gearbox of the acquisition vehicle, particularly on the more severe bends. As the model and video sequences were controlled through the accelerator pedal only, the time taken to change gears was not present in the model or the video sequences. The model also lacks geometric features that were not part of the mapped road, such as junctions. This may account for some differences between the reported average speeds in the three data sets.

An additional factor may have been that the driver of the mapping vehicle responded to the speed reported by the speedometer. The speedometer in the simulator was accurate; however, the speedometer of the acquisition vehicle was constrained by the manufacturer's calibration of it. The speedometer of a car can, because of legislation laid down by the European Union, report speeds up to 110% of the actual speed, but not lower (*33*). In addition, other factors, such as tire pressure, may have affected the accuracy of the reported speed.

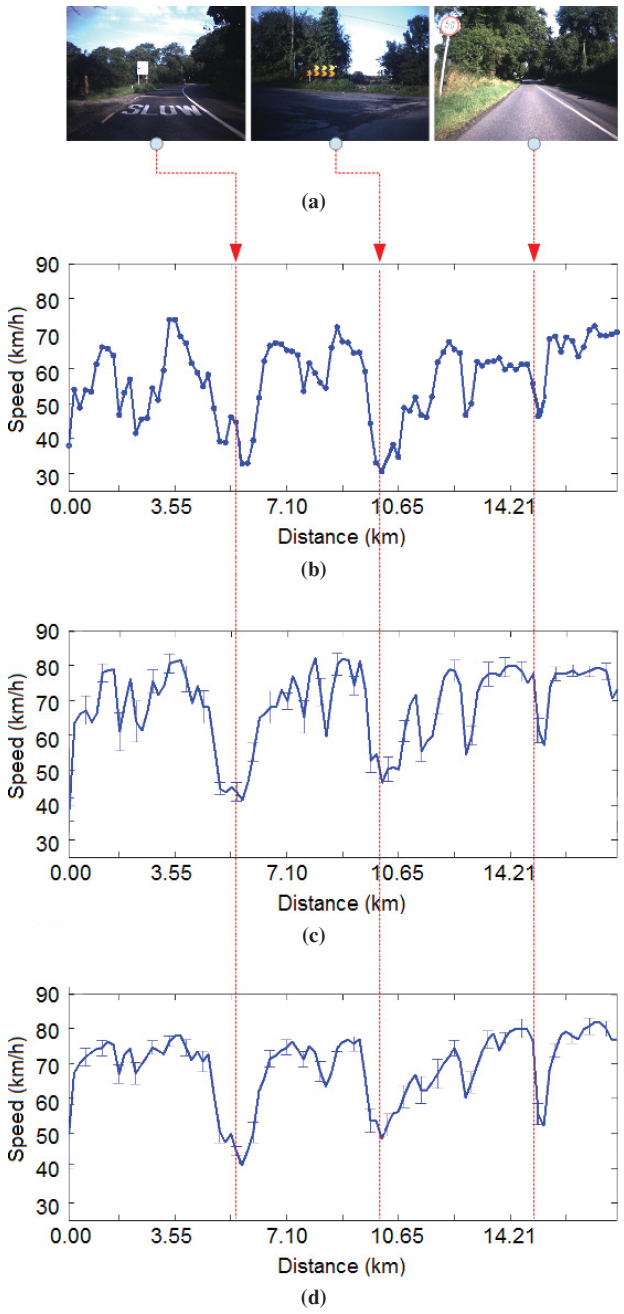

FIGURE 6 Features and average values of three data sets: (*a*) photos of features to reduce speeding, (*b*) ground truth average speed values, (*c*) video average speed values, and (*d*) model average speed values.

Reliability

Reliability is how the video and model relate to the ground truth. The Pearson product-moment correlation coefficient, *r,* between the ground truth and the video was calculated to be 84.6%, and the correlation between the ground truth and the model was calculated to be 87.3%. These correlation values were calculated across the entire route. This correlation was chosen because, although the data were nonlinear, it was expected that the relationship between the three data sets would be linear, as the three described speeds along the same route. As the average speed was recorded at the same position on the road for each of the three data sets, it was possible to correlate these data and thereby examine the similarity of the drivers' response in terms of speed to each of the different fidelities. The video and model are shown in Figure 6, *c* and *d.*

Validity

Validity is represented as the ability of the driving simulator to measure that which it was designed to measure. As participant reactions to both visual cue streams had a strong correlation, with an *r*-value between the video and model data of 92.8%, and each stream has a strong correlation with the ground truth, it has been shown that the driving simulator is a valid instrument with which to measure speed. Within the constraints of the on-the-rails visual cue streams, the human operators' judgment and management of the speed were comparable to those of the driver of the mapping system. The decreases and increases in speed, while not absolutely similar, were consistent with dangerous bends, features, and changes in posted speed limits. The lack of vestibular feedback may have been a factor in the differences. Another factor may have been that, because of the nature of the mapping system and the level of synchronization required, the ground truth data related to a single individual driving a road once, while the video and model sequences were the result for the 11 participants.

CONCLUSION

This paper has shown that a sparse graphical model can be constructed and populated with data acquired by a simple mobile mapping system. For a synchronized comparison of the model and video data, the steering component of the driving simulator was disabled to reflect the nonavailability of steering in the video sequence. A comparison of driver speed data, collected with the ground truth mapping system, and the video and model fidelities shows that the correlation between the video and ground truth was 84.6% and the correlation between the model and ground truth was 87.3%. The correlation between the video and the model driver speeds had a significant value of 92.8%.

The steering and vestibular systems present in high-fidelity driving simulators were absent from the simulator used during this evaluation work, so the influence of these factors on driver speed could not be measured. However, driver speed response to road features was consistent across the different fidelities, with participants reducing and increasing speed at the same points in each of the visual cue streams. The model did not contain the same complexity as the original road, so speed differences may have occurred when, for example, a junction was not included in the model.

Making an initial comparison between the model and video sequences required placing a constraint on the steering dynamics in the model. With this constraint, it has been shown that the speed between the video and model correlate, with differences being attributed to features present in the video but not the model. The next step in this work will be to introduce steering in the model and video sequences, where differences in speed may be observed and quantified, as the speed and steering responses have been separated.

It should also be noted that the steering of the driver during the road mapping process was recorded, in effect, by the inertial measurement unit, in terms of its yaw angle. A limited physics model

that adapts specific car models into the driving simulator has been developed and will be integrated into the driving simulator in the near future.

Future work will include incorporating steering dynamics into the video sequence, measurement of eye gaze, physiological responses, acceleration, braking, and user experience. Working prototypes of the video steering solution exist and are being integrated into the full-scale driving simulator.

ACKNOWLEDGMENTS

The authors thank the Irish Research Council for its continuing support and the participants for their time.

REFERENCES

1. Allen, R. W., T. J. Rosenthal, and M. L. Cook. A Short History of Driving Simulation. In *Handbook of Driving Simulation for Engineering, Medicine and Psychology* (D. L. Fisher, M. Rizzo, J. Caird, and J. D. Lee, eds.), CRC Press, Boca Raton, Fla., 2011, pp. 1–16.
2. Whelan, T., H. Johannsson, M. Kaess, J. J. Leonard, and J. McDonald. Robust Real-Time Visual Odometry for Dense RGB-D Mapping. Presented at IEEE International Conference on Robotics and Automation, Karlsruhe, Germany, 2013.
3. Izadi, S., D. Kim, O. Hilliges, D. Molyneaux, R. Newcombe, P. Kohli, J. Shotton, S. Hodges, D. Freeman, A. Davidson, and A. Fitzgibbon. KinectFusion: Real-Time 3D Reconstruction and Interaction Using a Moving Depth Camera. *ACM Symposium on User Interface Software and Technology (UIST),* Santa Barbara, California, 2011, pp. 559–568.
4. SCS Software. SCANIA Truck Driving Simulator. 2012.
5. Jia, L., S. Han, L. Wang, and H. Liu. Development and Realization of A Street Driving Simulator for Virtual Tour. *40th Annual Simulation Symposium (ANSS-40),* Norfolk, Va., 2007, pp. 133–136.
6. Lee, J. D., D. V. McGehee, J. L. Brown, C. M. Richard, O. Ahmad, N. J. Ward, S. Hallmark, and J. Lee. Matching Simulator Characteristics to Highway Design Problems. In *Transportation Research Record: Journal of the Transportation Research Board, No. 2248,* Transportation Research Board of the National Academies, Washington, D.C., 2011, pp. 53–60.
7. van der Horst, A. R. A., and J. H. Hogema. Driving Simulator Research on Safe Highway Design and Operation. In *Transportation Research Record: Journal of the Transportation Research Board, No. 2248,* Transportation Research Board of the National Academies, Washington, D.C., 2011, pp. 87–95.
8. Kuhn, W., I. Leithoff, and R. Kubik. Three-Dimensional Methodology for Design of Safe Rural Highways. In *Transportation Research Record: Journal of the Transportation Research Board, No. 2282,* Transportation Research Board of the National Academies, Washington, D.C., 2012, pp. 81–90.
9. OpenDrive.org. 2013. http://www.opendrive.org.
10. TopCon Mapping System. TopCon Positioning Systems, Inc. 2013. http://www.topconpositioning.com/products/mobile-mapping/ip-s2-hd.
11. Wilkie, D., J. Sewall, and M. C. Lin. Transforming GIS Data into Functional Road Models for Large-Scale Traffic Simulation. *IEEE Transactions on Visualisation and Computer Graphics,* Vol. 18, No. 6, 2012, pp. 890–901.
12. Google Earth. 2013. earth.google.com.
13. Open Street Map. 2013. http://openstreetmap.org.
14. Kaneswaran, D., et al. Replicating Reality: The Use of a Low Cost Driving Simulator for Design and Evaluation. *Proc., 24th IET Irish Signals and Systems Conference,* Letterkenny, Donegal, Ireland, 2013, pp. 29–35.
15. GeoQuake. 3D Driving Simulator on Google Earth. 2013. http://www.geoquake.com/drivingsimulator/earth/.
16. Ono, S., M. Kagesawa, H. Kawasaki, M. Onuki, J. Abeki, T. Yano, M. Nerio, K. Honda, and K. Ikeuchi. A Photo-Realistic Driving Simulation System for Mixed-Reality Traffic Experiment Space. *IEEE Symposium on Intelligent Vehicles,* Las Vegas, Nev., 2005, IEEE, New York, pp. 747–752.
17. Bredif, M. Image-Based Rendering of LOD1 3D City Models for Traffic-Augmented Immersive Street-View Navigation. *ISPRS Annals of the Photogrammetry, Remote Sensing and Spatial Information Sciences, Volume II-3/W3,* Antalya, Turkey, International Society for Photogrammetry and Remote Sensing, 2013.
18. Divekar, G., A. K. Pradhan, A. Pollatsek, and D. L. Fisher. Effect of External Distractions: Behavior and Vehicle Control of Novice and Experienced Drivers Evaluated. In *Transportation Research Record: Journal of the Transportation Research Board, No. 2321,* Transportation Research Board of the National Academies, Washington, D.C., 2012, pp. 15–22.
19. Elvik, R. Effects of Mobile Phone Use on Accident Risk: Problems of Meta-Analysis When Studies Are Few and Bad. In *Transportation Research Record: Journal of the Transportation Research Board, No. 2236,* Transportation Research Board of the National Academies, Washington, D.C., 2011, pp. 20–26.
20. Fitzpatrick, K., S. T. Chrysler, E. S. Park, V. Iragavarapu, and A. A. Nelson. Driver Performance at High Speeds Using a Simulator. In *Transportation Research Record: Journal of the Transportation Research Board, No. 2321,* Transportation Research Board of the National Academies, Washington, D.C., 2012, pp. 88–97.
21. Hoffman, J. D., J. D. Lee, T. L. Brown, and D. V. McGehee. Comparison of Driver Braking Responses in a High-Fidelity Simulator and on a Test Track. In *Transportation Research Record: Journal of the Transportation Research Board, No. 1803,* Transportation Research Board of the National Academies, Washington, D.C., 2002, pp. 59–65.
22. Blana, E. *Driving Simulator Validation Studies: A Literature Review*. Working Paper 480. Institute of Transport Studies, Leeds, United Kingdom, 1996.
23. Allen, R. W., G. D. Park, and M. L. Cook. Simulator Fidelity and Validity in a Transfer-of-Training Context. In *Transportation Research Record: Journal of the Transportation Research Board, No. 2185,* Transportation Research Board of the National Academies, Washington, D.C., 2010, pp. 40–47.
24. Logitech. Logitech G27 Racing Wheel. 2013. http://gaming.logitech.com/en-roeu/product/g27-racing-wheel.
25. Matrox. Matrox: TripleHead2Go. 2013. http://www.matrox.com/graphics/en/products/gxm/th2go/displayport/.
26. National Roads Authority Ireland (NRA). 2013. http://www.nra.ie/.
27. Point Grey Research. Bumblebee XB3. 2013. http://www.ptgrey.com/products/bbxb3/.
28. NovAtel. NovAtel: Pro-Pak V3. 2013. http://www.novatel.com/products/gnss-receivers/enclosures/propak-v3.
29. Brogan, M., S. McLoughlin, and C. Deegan. Assessment of Stereo Camera Calibration Techniques for a Portable Mobile Mapping System. *IET Journal of Computer Vision,* Vol. 7, No. 3, 2013, pp. 209–217.
30. Haughey, S., M. Brogan, S. Murray, C. Deegan, C. Fitzgerald, and S. McLoughlin. Sensor Integration for Mobile Mapping and Feature Analysis. *Proc., Road Transport Information and Control (RTIC) Conference,* London, 2010.
31. McLoughlin, S., C. Deegan, C. Mulvihill, C. Fitzgerald, and C. Markham. Mobile Mapping System for the Automated Analysis of Road Signage and Delineation. *IET Intelligent Transport Systems,* Vol. 2, 2008, pp. 61–73.
32. Scaramuzza, D., and F. Fraundorfer. Visual Odometry [Tutorial]. *IEEE Robotics and Automation Magazine,* Vol. 18, No. 4, 2011, pp. 80–92.
33. Legislation.gov.uk. *Statutory Instruments 2001 No. 25, The Motor Vehicles (Approval) Regulations 2001,* p. 37. http://www.legislation.gov.uk/uksi/2001/25/pdfs/uksi_20010025_en.pdf.

The Simulation and Measurement of Vehicle and Operator Performance Committee peer-reviewed this paper.